Geophys. J. Int. (2009) **176,** 555–564 doi: 10.1111/j.1365-246X.2008.03986.x

The source-box wave propagation hybrid methods: general formulation and implementation

I. Opršal,[1,2] C. Matyska[2] and K. Irikura[3]

[1]*Disaster Prevention Research Institute DPRI, Kyoto University, Gokasho, Uji, Kyoto* 611-0011, *Japan. E-mail: Ivo.Oprsal@mff.cuni.cz*
[2]*Charles University, Faculty of Mathematics and Physics, Department of Geophysics, V Holešovičkách* 2, 180 00 *Prague* 8, *Czech Republic*
[3]*Aichi Institute of Technology, Faculty of Engineering, Department of Urban Environment, Disaster Prevention Research Center,* 1247 *Yachigusa, Hachikusacyo, Toyota, Aichi* 470-0392, *Japan*

Accepted 2008 September 18. Received 2008 September 18; in original form 2007 August 29

SUMMARY

Originated by Alterman and Karal (AK) in 1968 as a domain-coupling technical algorithm, the generalized hybrid approach of wave injection is described by binding two subvolumes treated per partes by arbitrary wave-propagation methods. The generalized AK two-step procedure combines the source and path effects computed by one arbitrary method and local site effects computed by another (arbitrary) method using the first method's wavefield as input. The advantage of the approach arises from the fact that the connection between the methods keeps the formal wave-injection boundary perfectly permeable for the wavefield scattered by local structure and can be applied to a variety of hybrid formulations. This hybrid approach leads to more effective modelling of combined source, path and site effects (e.g. by multiple second-step computations with varying structure, using single first step input), thereby reducing computer memory and time requirements. The main innovation of the paper is the generalization of the boundary condition acting between two complementary subvolumes of AK hybrid wave-propagation methods.

Key words: Site effects; Computational seismology; Wave propagation.

1 INTRODUCTION

This paper summarizes and unifies the approaches developed subsequent to the introduction of the source box method (Alterman & Karal 1968), conveying their universal nature. This is introduced by defining independent wavefields for identical sources and regional structures, but different local structures. It will quickly become apparent that such an approach, covering a wide range of implementations, leads to the description of simple conditions introduced by (Alterman & Karal 1968) or to conditions for structure adjacent to the free surface given in Bielak & Christiano (1984), for example.

Recently, hybrid modelling in 3-D wave-propagation methods has grown in its importance. Using a combination of the methods is often a necessity due to limited computational and temporal capacity. Hybrid wave propagation modelling in seismology takes advantage of individually used methods (with e.g. source path and site effects computed consequently), while accounting for complete source-path-site effects. The main benefits against all-in-one methods are not only the combination of the advantages of the methods, but also increasing the algorithmic efficiency in computing sophisticated, or previously uncomputable, problems. A number of various approaches is mentioned in, for example; Moczo *et al.* (2007a,b), Opršal *et al.* (2002) and Opršal & Zahradník (2002). This applies also for the cases where lower-order methods are used at a free-surface vicinity (Hestholm *et al.* 2006) since the numerical dispersion of Rayleigh waves can be reduced only by finer spatial sampling, not by increasing the order of the method (Xu *et al.* 1999).

Here we concentrate on the wavefield injection approach which was probably introduced in the pioneering work of Alterman & Karal (1968), where separate computations are done due to a source singularity in finite-difference (FD) computations. The singularity was avoided by computing the exact wavefield for the source in a full space and by computation of the wave propagation in the original volume, subdivided into a part enveloping the original source subvolume and its complement. Different wavefields, satisfying the same elastodynamic equation, were computed in each of the complements, with algorithmic FD coupling on the boundary between them. The term 'wave injection' was introduced by Robertsson & Chapman (2000).

The AK-type approaches allow for 'perfect' connection between the background and complete wavefield domains, but still, the methods use the principle in a way tailored to an applied numerical approach without showing any boundary condition in general. However, the approaches may be unified by the general boundary condition applied on the excitation box (EB) (eqs 6–9). The thought of a rigorously described boundary condition thus came as a need to simply unify the many applied combinations by boundary conditions applied at the EB. The reasons are not only scientific but

© 2008 The Authors
Journal compilation © 2008 RAS

also educational—the tailored implementation may be more difficult to understand than the general description that does not require a detailed knowledge of methods used in a particular combination, especially in cases where the wavefield injection is not fully theoretically justified, but implemented in a purely technical way.

The objective of this paper is twofold: (i) to generally formulate a condition on the boundary between the two complementary parts of the wave propagation volume and (ii) to discuss some specifics of implementation.

2 THE METHOD

2.1 General conditions for linear elastic case

Let us consider two independent cases of 3-D-inhomogeneous linear elastic media B and C, respectively, extending in the full space (see Figs 1 and 2). The media B and C are identical except for a volume of finite dimensions (difference volume DV) completely encompassed by a surface called the excitation box, where intersection $EB \cap DV = \emptyset$. General voluminal source S is formally represented by forces $\vec{S}$ in the elastodynamic equation. Let EB and S be identically positioned in both B and C medium, with respect to DV. Let $\vec{u}_b$ be the displacement of the wavefield (called the background wavefield) due to the source S in the medium B, and $\vec{u}_c$ be the displacement of the wavefield (called the complete wavefield) due to the (same) general source S in the medium C. We thus deal with two separated wavefields, which are generated by the same source but propagate in two different infinite media.

Both fields $\vec{u}_b$ and $\vec{u}_c$ are physical quantities satisfying the elastodynamic equations. These equations are identical outside the EB but may differ inside the EB if there are different material properties; that is,

$$\mathcal{L}_c(\vec{u}_c) + \vec{S} = 0, \tag{1}$$

$$\mathcal{L}_b(\vec{u}_b) + \vec{S} = 0, \tag{2}$$

$$\mathcal{L}_c = \mathcal{L}_b \equiv \mathcal{L} \quad \text{outside the EB and on the EB} \quad (\text{because EB} \cap DV = \emptyset), \tag{3}$$

where $\mathcal{L}_c(\mathcal{L}_b)$ are linear differential operators and $\vec{S}$ is a source function, which depends on spatial variables and time (or frequency, if the eqs (1) and (2) are considered in the frequency domain). In general, the source has finite dimensions and the function $\vec{S}$ may be

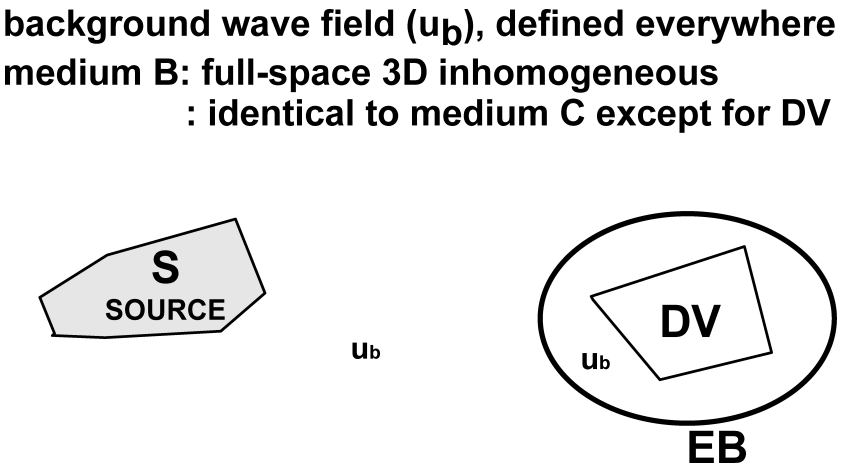

Figure 1. Background wavefield—solution to eq. (2). Voluminal source S in 3-D-inhomogeneous linear elastic medium B generates displacement u_b called background displacement, . The interior volume enclosed by the EB includes difference volume DV where the media C and B differ; thus C and B are identical elsewhere. The source S, the EB, and their constellation are identical in both B and C medium (see Fig. 2). The source S is placed outside the EB.

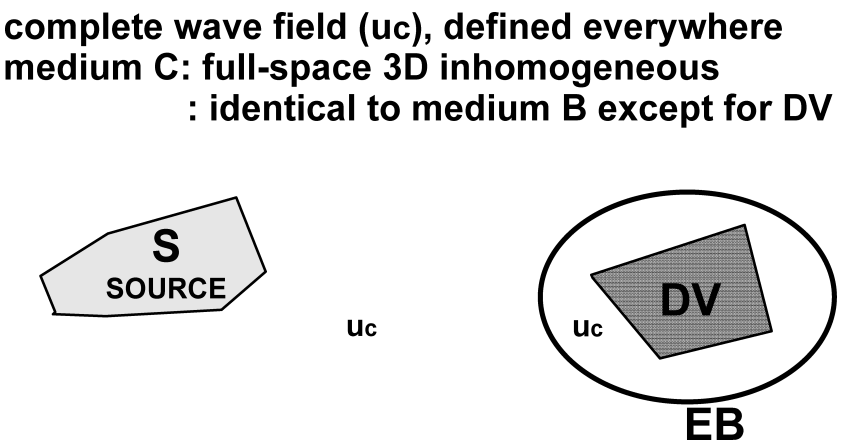

Figure 2. Complete wavefield—solution to eq. (1). Voluminal source S in 3-D-inhomogeneous linear elastic medium C generates displacement u_c called complete displacement. The interior volume enclosed by the EB includes difference volume DV where the media C and B differ; thus C and B are identical elsewhere. The source S, the EB, and their constellation are identical in both B and C medium (see Fig. 1). The source S is placed outside the EB.

© 2008 The Authors, *GJI*, **176,** 555–564
Journal compilation © 2008 RAS

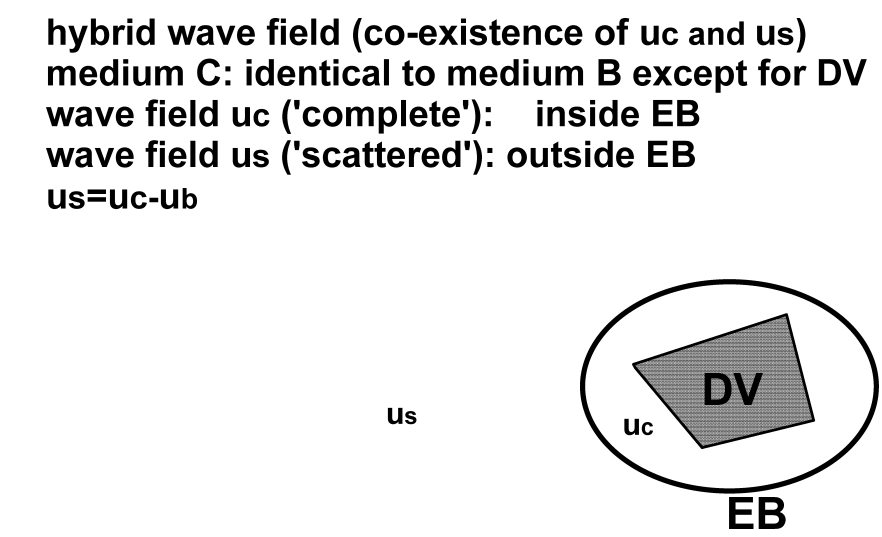

Figure 3. Hybrid wavefield. Outside the excitation box EB, there is a difference of the eqs (1) and (2) equivalent to (3), with the source term zeroed. The wavefields outside the EB is then $\vec{u}_s = \vec{u}_c - \vec{u}_b$. Complete wavefield $\vec{u}_c$ (eq. 1) is kept inside the EB. (see Figs 1 and 2).

non-zero both outside and inside the EB (Figs 1 and 2). The symbol $\equiv$ is used to denote definitions throughout the text. We assume that the displacement as well as the traction of both fields are continuous on the EB.

Let us introduce an auxiliary quantity, called the scattered wavefield ($\vec{u}_s$), defined by the difference:

$$\vec{u}_s \equiv \vec{u}_c - \vec{u}_b. \tag{4}$$

It is then possible to formally express a co-existence of two wavefields, so called hybrid wavefield, in the full space filled by the medium C (Fig. 3): The scattered wavefield $\vec{u}_s$ propagates in part of the 3-D infinite volume outside the EB (thus outside the DV, where medium C = B), and the complete wavefield $\vec{u}_c$ propagates inside the EB. The discontinuity of the hybrid wavefield on the EB, where fields $\vec{u}_b$, $\vec{u}_c$ and $\vec{u}_s$ are defined for structure C, is equal to $\vec{u}_b$ (4). While considering the co-existence of $\vec{u}_c$ and $\vec{u}_s$ in one medium (C), it is necessary to introduce boundary conditions for $\vec{u}_c$ and $\vec{u}_s$ on the EB.

By subtracting (2) from (1) and taking into account (3) we get

$$0 = \mathcal{L}_c(\vec{u}_c) - \mathcal{L}_b(\vec{u}_b) = \mathcal{L}(\vec{u}_c) - \mathcal{L}(\vec{u}_b) = \mathcal{L}(\vec{u}_c - \vec{u}_b) = \mathcal{L}(\vec{u}_s) \tag{5}$$

outside the EB, assuming the background wavefield $\vec{u}_b$ is known. In general, we do not have an equation for $\vec{u}_s$ inside the EB because $\mathcal{L}_c \neq \mathcal{L}_b$ if the media B and C differ inside the EB.

The main idea of the hybrid approach is to solve first the eq. (2) $[\mathcal{L}_b(\vec{u}_b) + \vec{S} = 0]$ in the whole space in the medium B (Fig. 1). The medium B is achieved by removing complex details from 'the real' medium C within the volume inside the EB. In practice, such a simplification would allow to use a less demanding numerical (or even analytical) method to evaluate the $\vec{u}_b$. The time history $\vec{u}_b$ on the EB is saved. After that, the elastodynamic eqs (5) ($\mathcal{L}(\vec{u}_s) = 0$) outside the EB, (1) $[\mathcal{L}_c(\vec{u}_c) + \vec{S} = 0]$ inside the EB and boundary condition on EB (using already known $\vec{u}_b$) are evaluated in medium C (Fig. 2). Special numerical techniques can be applied to be able to model correctly the wavefield complexities in the medium C. In usual applications, $\vec{S} = 0$ inside the EB and then $\mathcal{L}_c(\vec{u}_c) = 0$ is usually solved inside the EB. Outside the EB the sacttered wavefield would be again a solution to the elastodynamic equation, while identical source terms $\vec{S}$ in B and C media $\vec{S}$ would vanish (due to the subtraction). The temporally and spatially dependent discontinuity between the complete wavefield $\vec{u}_c$ inside the EB and the scattered wavefield $\vec{u}_s$ outside the EB is equal to the background wavefield $\vec{u}_b$. The boundary condition between $\vec{u}_c$ and $\vec{u}_s$ on the EB can be used to describe the boundary condition between the $\vec{u}_s$ and the $\vec{u}_c$ on the EB. Such a condition, representing the wavefield due to subtracted sources outside the EB, relates $\vec{u}_c$ on the inner (positive) side of the EB with $\vec{u}_s$ on the outer (negative) side of the EB. As the relation (4) is valid on the outside part of the EB and both $\vec{u}_c$ and $\vec{u}_b$ are continuous on the EB, we may write

$$[\vec{u}] \equiv \vec{u}_c^+ - \vec{u}_s^- = \vec{u}_c^+ - \vec{u}_c^- + \vec{u}_b^- = \vec{u}_b^- = \vec{u}_b^+ \equiv \vec{u}_b^{EB}. \tag{6}$$

The practical use of boundary condition on the EB in hybrid wavefield computation given by eq. (6), for example, consists of ability to evaluate an immediate value of $\vec{u}_c^+$ (inner side of the EB) from immediate value of displacement $\vec{u}_s^-$ (outer side of the EB) by adding $\vec{u}_b^{EB}$ (known from $\vec{u}_b$ computation—Fig. 1) and vice versa. The boundary condition on the EB for $\vec{u}_c$ and $\vec{u}_s$, respectively, can be expressed by re-arranging (6) into a form

$$\vec{u}_c^+ = \vec{u}_s^- + \vec{u}_b^{EB} \qquad \text{and} \quad \vec{u}_s^- = \vec{u}_c^+ - \vec{u}_b^{EB}. \tag{7}$$

Wavefields $\vec{u}_s$ and $\vec{u}_c$ are evaluated simultaneously, typically by one method, outside and inside the EB, respectively. The background wavefield $\vec{u}_b^{EB}$ (due to source S) generates the $\vec{u}_c$ and $\vec{u}_s$ via boundary condition (7). This is exactly equivalent (in FD sense) to the original finite-difference formulation of Alterman & Karal (1968) (fig. 6, eqs 35), where only displacements are used.

Since we take into account the linear elasticity only, the stress tensor $\vec{\sigma}_s$ of the scattered field can be introduced as the difference between the stress tensors of the complete and background fields outside the EB. By analogy to displacement we can write for the stress tensor:

$$[\vec{\sigma}] \equiv \vec{\sigma}_c^+ - \vec{\sigma}_s^- = \vec{\sigma}_c^+ - \vec{\sigma}_c^- + \vec{\sigma}_b^-. \tag{8}$$

The difference between the traction $\vec{T}_c^+$ of the complete field to the positive side of the EB and the traction $\vec{T}_s^-$ of the scattered field to the negative side of the EB is then similarly expressed as:

$$[\vec{T}] \equiv \vec{T}_c^+ - \vec{T}_s^- = \vec{T}_c^+ - \vec{T}_c^- + \vec{T}_b^- = \vec{T}_b^- = \vec{T}_b^+ \equiv \vec{T}_b^{EB}, \tag{9}$$

because the traction of both the complete and the background fields are continuous on the EB. These conditions are identical to part of

© 2008 The Authors, *GJI*, **176,** 555–564
Journal compilation © 2008 RAS

conditions written by Bielak & Christiano (1984) to bind wavefields in cases of a structure adjacent to a free surface and an absent structure, respectively. Our formulation, based on looking at the difference between wavefields of two independent cases, includes the possibility of a free surface intersecting the EB as a subset solution.

The background $\vec{u}_b$ and complete $\vec{u}_c$ fields are continuous in full 3-D volume, excited by the original source function $\vec{S}$—see eqs (2 and 1), respectively. However, the hybrid field composed by both, $\vec{u}_s$ outside the EB and $\vec{u}_c$ inside the EB, hereafter denoted by $\vec{u}$, is, in principle, discontinuous.

The EB does not impose any effect to $\vec{u}_s$ because of linear rheology, when the scattered wavefield $\vec{u}_s$ is perfectly separable from $\vec{u}_c$ on EB. Hence the EB is perfectly permeable for the scattered wavefield $\vec{u}_s$. More generally: The EB is permeable for any wavefield linearly added to the $\vec{u}_b$ solution according to actual linear rheology on the EB.

Now let the generally discontinuous wavefield $\vec{u}$ be re-arranged as follows:

$$\vec{u} = \vec{u}_c \quad \text{inside EB,} \qquad \vec{u} = \vec{u}_s \quad \text{outside EB.} \tag{10}$$

Then everywhere, excluding EB, $\vec{u}$ obeys the equation:

$$\mathcal{L}_c(\vec{u}) = 0, \tag{11}$$

and

$$[\vec{u}] = \vec{u}_b^{EB} \ , \ [\vec{T}] = \vec{T}_b^{EB} \tag{12}$$

on EB, while $\vec{u}_b$ obeys

$$\mathcal{L}_b(\vec{u}_b) + \vec{S} = 0 \tag{13}$$

everywhere, including the EB. Hence we have an equation of motion for the discontinuous wavefield $\vec{u}$ with one boundary condition and one additional equation for $\vec{u}_b$.

2.2 Method overview and generalization

We can thus summarize (see also Fig. 3): We want to solve eq. (1); the difficult 'all-in-one' problem, involving both the source effect and effects of the heterogeneities inside the EB. Instead, in the first step, we solve the equation for the background field, with the source, but with a simplified heterogeneity. The background field time history only on the EB is needed further. Then, in the second step, we solve simultaneously the elastodynamic equation without sources for the scattered field outside the EB and the equation for the complete field inside the EB, and we couple these fields by means of the boundary conditions (6), (7) and (9).

Note that the approach described in this section can be applied to all problems enabling the spatial decomposition by means of the excitation box with linear relations (5) satisfied outside the EB. Therefore, it is not necessary to deal only with the elastic rheology—we can use more general linear rheologies outside the DV, still being able to linearly separate $\mathcal{L}(\vec{u}_x) = 0$ and $\mathcal{L}(\vec{u}_c) = 0$ on the EB. Added to that, computation of the complete wavefield (or better, particle motion) inside the EB allows for use of general linear rheologies (even non-linear behaviour) inside the DV without loss of generality (see also Bielak & Christiano 1984).

2.3 Replication test

As a special case for checking purposes, let the media in B and C be identical while computing the $\vec{u}_b$ (Fig. 1) and $\vec{u}_c$ (Fig. 2) wavefields, respectively. Then complete wavefield

$$\vec{u}_c = \vec{u}_b, \tag{14}$$

and the scattered wavefield

$$\vec{u}_s = \vec{u}_c - \vec{u}_b = 0. \tag{15}$$

are called replication wavefields. Consequently, during the hybrid wavefield computation (Fig. 3), the scattered wavefield $\vec{u}_s$ computed outside the EB is zero by definition, and at the same time the complete wavefield $\vec{u}_c$ inside the EB is equal to $\vec{u}_b$.

2.4 Practical application of the hybrid approach

Practically the hybrid method computation is subdivided into two steps: In the first step $\vec{u}_b$ due to source S is computed in medium B and its values on the EB are saved. After that, in the second step, the complete wavefield $\vec{u}_c$ is computed in the interior of the EB and $\vec{u}_s$ outside the EB, all in the medium C. The advantage is that the volume of the second step can be truncated into a finite volume containing the EB and its close vicinity, typically without a strong impact on the complete wavefield. Hence the computational domain for this second step may be significantly reduced.

From now on, by hybrid approach we mean a two-step technique that attempts to compute separately the background wavefield ($\vec{u}_b$; Fig. 1) in the first step and hybrid wavefield ($\vec{u}_b, \vec{u}_c$; Fig. 3) in the second step. The future area of interest is enveloped by the EB. The $\vec{u}_b$ is recorded on the EB and saved ($\vec{u}_b^{EB}$). In the second step, the structure is added into the area of interest (inside EB, changing the structure to C). After that the saved background wavefield $\vec{u}_b^{EB}$ is used in 'implemented' boundary conditions on the EB to generate the wavefield as if it was entering the EB from outside. Consequently the $\vec{u}_c$ and $\vec{u}_s$ wavefields are computed.

For example, wave-propagation method used in the second step is applied in the whole volume to solve the elastodynamic equation by integration in time domain. The initial conditions for time $T = 0$: $\vec{u}_c = \vec{u}_s = \vec{u}_b = 0$. As given by eqs (10) and (11), $\vec{u}_c$ is evaluated inside and $\vec{u}_s$ outside of the EB. If the wavefield is evaluated on the EB (solving $\mathcal{L}_b(\vec{u}_b^{EB}) = 0$), then it can either provide the $\vec{u}_c^{EB}$ by $\mathcal{L}(\vec{u}_s^- + \vec{u}_b^{EB})$ or the $\vec{u}_s^{EB}$ by $\mathcal{L}(\vec{u}_c^+ - \vec{u}_b^{EB})$ (eqs 3 and 7) to represent either boundary value for the $\vec{u}_c$ inside the EB or $\vec{u}_s$ outside the EB, respectively. Hence the wavefield $\vec{u}_c$ propagates inside the EB and is equal to $\vec{u}_b$ until it reaches DV. If the structure inside the DV is different from B, then $\vec{u}_c \neq \vec{u}_b$ and such reflected $\vec{u}_c$ propagates (besides other directions) to the EB where it is subtracted the $\vec{u}_b$ (eq. 7) component and propagates outside the EB as $\vec{u}_s$. Hence $\vec{u}_s$ is zero (eq. 7) until first reflection from local changed structure arrives from inside the EB.

Computation of the replication wavefields ($\vec{u}_c, \vec{u}_s$) in the second hybrid step is called a 'replication test'. It gives wavefield $\vec{u}_c$ as being identical to the first step $\vec{u}_b$ in the whole interior of the EB and zero $\vec{u}_s$ in its exterior (see eqs 14 and 15)

For practical use it means that the structure of interest (the local structure) is to be always within the EB interior. Then the replication test of the hybrid method is the way to check the correctness of the wavefield injection. If the second-step structure is added to perform the computation, then the complete wavefield inside the EB is the same as if computed by the all-in-one method. At the same time, the scattered wavefield outside the EB is equal to the all-in-one fine-structure wavefield minus the first-step (background) wavefield. For more details see chapters 3.1, 3.2 and 3.3 of Opršal & Zahradník (2002).

2.5 Implementations of the hybrid approach in literature

In principle, the two-step AK coupling allows for a combination of arbitrary methods suitable to compute the wavefield generation and propagation, for example FD, the discrete wave number (DW) method, the ray theory (RT) method, finite elements (FE) or analytical solution.

Alterman & Karal (1968), who used 2-D source wavefield (the first step) injection into the 2-D FD computation (the second step), were followed by a variety of approaches. Some of them were equivalent to AK, while others were just 'very close' to their principle.

In the following text we use *SH* and *P–SV* abbreviations for scalar and vector wavefields; and for example, DW–FD for using the DW in the first step and the FD in the second step of the hybrid computation. The dimension, type of wavefield and the method used are given respectively for some of the listed methods (e.g. '; 2-D *P-SV* DW–FD').

For equivalent formulation (eq. 6) combining various 1-D and/or 2-D methods see also: Kelly *et al.* (1976, 2d FD-FD), Levander (1989; 2-D source-2D FD, 3-D source-2D FD), Zahradník & Moczo (1996; 2-D DW–FD planar free surface), Moczo *et al.* (1997; 2-D P-SV DW–FD hybrid connection; free surface topography treated by non-AK-like connected FE), Opršal *et al.* (1998; DW–FD), Opršal *et al.* (1999; 2D RT-FD), Fäh & Suhadolc (1994; 2-D modal summation-FD), Fäh *et al.* (1994; 2-D modal summation-FD), Moczo (1989, 2-D *SH* FD), Caserta *et al.* (1999; 2-D DW–FD topography models, stochastically perturbed excitation), Riepl (1997; 2-D DW–FD), Riepl *et al.* (2000; 2-D DW–FD), Fäh (1992), Fäh *et al.* (1990, 1993; 2-D modal summation-FD).

While Fäh *et al.* (1994; propagation from 3-D point source by modal summation - 2-D FD) used the coupling at vertical line subdividing the 'source' and 'site' quarter spaces, Zahradník (1995) suggested the extension to envelope the site of interest inside the excitation box, hence reversing the approach of AK using their principle.

Zahradník & Moczo (1996; DW–FD) and many others have followed (eqs 6–9): Robertsson *et al.* (1996; acoustic/viscoelastic 2-D Gaussian beam-FD, fourth order, staggered FD); Robertsson & Chapman (2000; 2-D FD-FD staggered grid), Robertsson *et al.* (2000; 2-D FD-FD staggered grid, 'wave injection'), Hatayama et al.(2000; DW(3-D)-FD(2-D staggered-grid P-SV). Equivalent to AK is also method of Takeuchi & Geller (2003), provided the analytic solution for an infinite medium is used in first step and use the conventional numerical operators (such as FD or FEM) are used in the second step of the hybrid computation (see also Takeuchi 1996).

The following papers present the source box method with line-to-point source technique mapping the wavefield from 2-D to 2.5D, hence taking into account the spreading over 3-D space instead of 2-D space: Vidale & Helmberger (1987, 1988), Helmberger & Vidale (1988) with fourth-order 2-D FD *P-SV*, Vidale *et al.* (1985, 2-D SH), Pitarka *et al.* (1994, 2-D SH), Pitarka *et al.* (1996, 2-D P-SV), Pitarka *et al.* (1996, 2-D FD second-order SH, 2-D fourth order staggered P-SV).

Takenaka *et al.* (2006) used 1-D FD plane-wave incidence excitation in 2-D or 2.5D FD hybrid computations to eliminate the spurious reflection from the boundaries.

A combination of full 3-D wavefield methods was recently presented by Opršal & Zahradník (2002; FD–FD), Opršal *et al.* (2002; 3-D RT-FD, DW–FD), Opršal *et al.* (2004; 3-D finite-extent source PEXT–FD), Opršal *et al.* (2005; pseudodynamic source DW–FD), Opršal & Fäh (2007, analytical-FD; modal summation-FD), Fäh *et al.* (2006; analytical-FD; modal summation-FD) and Sorensen *et al.* (2006; DW–FD).

Hatayama (2006) combines modal summation (Love and Rayleigh waves) and 3-D staggered grid FD (velocity stress formulation) but unlike, for example, Robertsson *et al.* (2000) the discontinuity on the border is applied only in velocities, not in stresses (L. Eisner, personal communication, 2007).

The two-step approach applied in the 2-D FE modelling was developed theoretically for structure adjacent to the free surface by Bielak & Christiano (1984), preceded by Herrera & Bielak (1977), and further followed by Loukakis (1988) and Cremonini *et al.* (1988), Gazetas *et al.* (2002). Recently, their method was extended to the 3-D FE-FE hybrid modelling as DRM (domain reduction method) by Bielak *et al.* (2003), Yoshimura (2003), Yoshimura *et al.* (2003), Yang *et al.* (2003), Bielak (2005), Faccioli *et al.* (2005), Stupazzini *et al.* (2006) and Kontoe *et al.* (2008a,b).

Lecomte (1996), Gjøystdal *et al.* (1998, 2002), Hokstad *et al.* (1998) and Lecomte *et al.* (2004) combined RT and FD (where RT is an asymptotic solution of the wave equation and 2-D FD can be elastic or acoustic). The FD is computed for a buried structure model and the scattered wavefield is then propagated to the free surface. The coupling technique, basically described in Lecomte (1996), makes the coupling line non-permeable, however, it can be turned into the Alterman & Karal (1968) treatment by a simple additional operation to fulfil eq. (6). After that, not only the coupling line becomes permeable for the scattered wavefield (see Section 2.1), but the wavefield above such a horizontal line would be only scattered ($\vec{u}_s$; eq. 4) by definition and therefore its propagation to the free surface via RT would also be possible for an arbitrarily long excitation signal. Hence the RT-FD-RT technique of Lecomte *et al.* (2004) can be added to the group of methods describable by the Alterman & Karal (1968) principle.

Close to the AK method is the paraxial approach of De Martin *et al.* (2007) and Modaressi (1987) who use FD-FE, where the excitation field is extracted from FD by the paraxial approximation technique applied at the excitation boundary. The scattered wavefield is then absorbed at the boundary, again using the paraxial approximation. In principle, the absorbed wavefield may also be further propagated outside the complete wavefield area in a case of need. The disadvantage of paraxial approximation is lower accuracy in comparison with the AK approach, especially in heterogeneous medium whereas the FD-FD AK method is practically exact in terms of injection, producing only truncation, or possibly interpolation errors (see more in Section 2.5.3). However, the approach can also be applied inside Non-linear medium (Bamberger *et al.* 1986) where directly employing the AK method fails. The failure of directly using the AK method is due to the necessity to maintain time dependent discontinuity of the wavefield on the EB which is being added or subtracted from the so called scattered or complete wavefields, see (6).

2.5.1 Boundary conditions on EB

The second step of the hybrid computation evaluates by a single method hybrid wavefield composed of two different wavefields: the $\vec{u}_c$ inside and the $\vec{u}_s$ outside the EB. Both co-existing fields are continuous except for their border, the EB. The boundary condition between these wavefields is expressed by using the previously computed background wavefield and is the only source generating the hybrid wavefield. It depends on the actual method used as how to apply the quantities given in eqs (6)–(9). For example,

© 2008 The Authors, *GJI*, **176,** 555–564
Journal compilation © 2008 RAS

for purely single-quantity methods, such as the displacement formulation (e.g. Alterman & Karal 1968; Moczo 1989; Opršal & Zahradník 2002), choose the EB to be approximated by adjacent grid lines (gridpoints) of the FD grid. The two lines (for second-order methods) are inside ($\vec{u}_c$ values) and outside ($\vec{u}_s$ values) the EB, respectively. The $\vec{u}_b$ is recorded for gridpoints on both of these grid lines and then subtracted or added to the actually computed displacements needed by a FD stencil that is centered on one of the two adjacent grid lines. For instance, an FD computing $\vec{u}_c$ is in the vicinity of the EB (centered inside the EB). Some of the stencil gridpoints, however, are situated outside the EB and have instant values of the $\vec{u}_s$. The instant values of $\vec{u}_s$ at these points neighbouring the EB can be added the known values of the $\vec{u}_b$ corresponding to an actual time t. It can be expressed by differentiation of the eq. (7, left) as $\vec{u}_c^{\,\mathrm{GPIEB}}(t) = \vec{u}_s^{\,\mathrm{GPOEB}}(t) + \vec{u}_b^{\,\mathrm{GPOEB}}(t)$, where GPIEB, GPOEB means 'gridpoint inside the EB' and 'gridpoint inside the EB', respectively. It appears after some algebra (not shown here) that the above mentioned application of the displacement discontinuity $[\vec{u}] = \vec{u}_b$) on two neighbouring grid lines in FD displacement formulation is equivalent to applying the traction discontinuity $[\vec{T}] = \vec{T}_b$ (see eq. 20) applied between the $\vec{u}_s$ and $\vec{u}_c$ grid lines, hence located at the position of the 'theoretical' EB.

In cases of stress-velocity FD formulations, the velocity and stress discontinuities are used (e.g. Robertsson & Chapman 2000; Robertsson *et al.* 2000).

Quantities additionally required by a given hybrid method (e.g. in DW–FD (staggered) or FE–SE template), but not stored as the background field, can be computed from the background field by using known rheology and background structure. For example Hatayama (2006) applies the discontinuity only in velocities, not in stresses that can be computed from the known background and complete velocity wavefield, rheology, and structure. However, the accuracy of such an approach can be affected. It was also applied in Loukakis & Bielak (1994), where the need to store the traction discontinuities (Bielak & Christiano 1984, also effective forces in equivalent source approach of Faccioli *et al.* 2004) can be avoided by storing discontinuities at the belt between soil and structure (Bielak 2005). We do not go into details of particular implementations of the AK method by various authors since it is beyond the scope of this paper.

The next example shows a relationship between $[\vec{T}] = \vec{T}_b$ and $[\vec{u}] = \vec{u}_b$ for the elastic isotropic linear case, following relationships from Section 2.1. Let wavefields $\vec{u}_b$ (Fig. 1), $\vec{u}_c$ (Figs 2 and 3), and $\vec{u}_s$ (Fig. 3) be solutions to the same elastodynamic equation. Then

$$\vec{u}_s = \vec{u}_c - \vec{u}_b \,, \tag{16}$$

the background wavefield at EB is expressed as displacement discontinuity

$$[\vec{u}] = \vec{u}_c^{\,EB} - \vec{u}_s^{\,EB} = \vec{u}_b^{\,EB} \,, \tag{17}$$

Hooke operator gives rheology binding stress tensor σ with displacement (λ and μ being Lamé elastic coefficients):

$$H(\vec{u}) = \sigma = \lambda \nabla \cdot \vec{u} \bar{I} + \mu \left[\nabla \vec{u} + (\nabla \vec{u})^T \right] \,, \tag{18}$$

where $\bar{I}$ is identity tensor and

$$\sigma_i = H(\vec{u}_i) \,, \qquad i \in \{c, s, b\} \,. \tag{19}$$

Displacements and stress tensors at the EB can be written $\vec{u}_i^{\,EB}, \sigma_i^{\,EB},\ i \in \{c, s, b\}$. The traction discontinuity at the EB writes:

$$[\vec{T}] = [\sigma^{EB} \cdot \vec{n}] = \vec{T}_b^{\,EB} = (\sigma_c^{\,EB} - \sigma_s^{\,EB}) \cdot \vec{n} = \vec{T}_c^{\,+} - \vec{T}_s^{\,-} \tag{20}$$

inserting eqs (19) and (17) into (20):

$$[\vec{T}] = [H(\vec{u}_c^{\,EB} - \vec{u}_s^{\,EB})] \cdot \vec{n} = H(\vec{u}_b^{\,EB}) \cdot \vec{n} = H([\vec{u}] \cdot \vec{n}) \,, \tag{21}$$

where $\vec{n}$ is the normal vector to the EB boundary pointing into the interior of the EB (Fig. 4). After using (18) in (21) we get the traction discontinuity at the EB expressed by the known background displacement:

$$[\vec{T}] = \lambda \nabla \cdot \vec{u}_b^{\,EB} \bar{I} \cdot \vec{n} + \mu \left[\nabla \vec{u}_b^{\,EB} + (\nabla \vec{u}_b^{\,EB})^T \right] \cdot \vec{n} \,. \tag{22}$$

Eqs (17), (20) and (22) express the EB boundary conditions (here for the isotropic elastic medium). Again, there is no difference between the use of $\vec{u}, \dot{\vec{u}}, \ddot{\vec{u}}$ in eq. (17) nor in eqs (20)–(22) where $\vec{T}$ would have a meaning of $\dot{\vec{T}}$, and $\ddot{\vec{T}}$, respectively. It is in order to consider gradient of the background wavefield (such as $\nabla \vec{u}_b^{\,EB}$) on the EB because $\vec{u}_b$ is defined everywhere in the first step. If an interface (including the free surface) intersects the EB then the gradient can be understood either in the sense of a limit of a smooth medium, or a in a sense of a distribution. In practical use, it is trivial to record, during the first step of hybrid computation, all that is needed for the second-step computational method—for example, recording the values of the $\vec{u}_b$ at neighbouring FD gridpoints to get $\nabla \vec{u}_b^{\,EB}$.

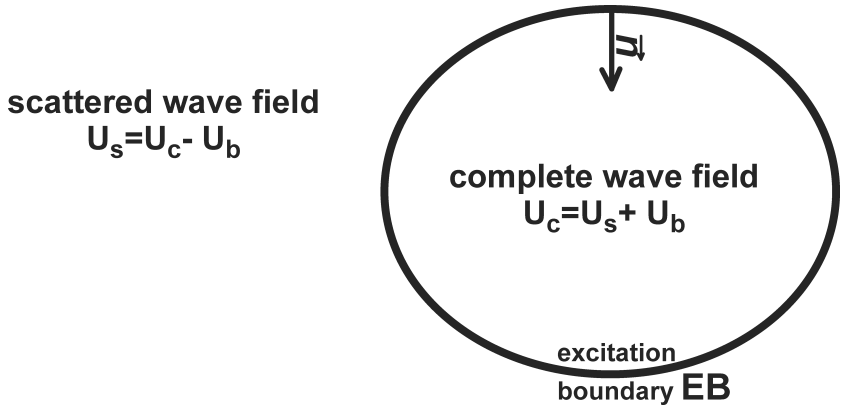

Figure 4. Second step of the hybrid method. The two wave-propagation domains coupled by generalized AK algorithm divided by the excitation boundary (EB) represented by the ellipse. The background wavefield (u_b) computed at the first step in whole volume is saved on the EB. In the second step, the EB-saved (u_b) then fully represents the wavefield from the first step. The complete (u_c) and scattered (u_s) wavefields are both computed in the second step inside and outside the EB, respectively.

2.5.2 choice of EB

The EB is typically chosen to encompass the local structure of interest with minimum voluminal requirements. Then the outside of the EB with further interfaces and inhomogeneities is usually truncated to minimize the computer memory and time requirements, and only the necessary volume is left for transparent boundaries or dampers.

The use of the cropped model (in the hybrid computation) limits the interactions between the inserted second-step local structure and the outer medium to the interaction with the contents of the incoming background wavefield $\vec{u}_b$—this wavefield may include, for example, surface waves and body waves influenced by the source, path and 3-D structure around the EB. As for the multiple reflections of scattered wavefield $\vec{u}_s$ between the inserted local structure inside the EB and the regional structure outside the EB, it can be modelled by enlarging the second-step computational model to include the outside structure (see e.g. Robertsson & Chapman 2000; Robertsson *et al.* 2000; Opršal & Zahradník 2002). This also puts a constraint on the 'independence of the second-step results on the first step model' (Opršal & Zahradník 2002, section 6.2.2, fig. 8) to cases with weak or smooth inhomogeneities, including cases when the outside structure is not present due to truncating the model to reduce computer memory requirements.

2.5.3 numerical accuracy and replication test

The replication test allows us to check the binding approximation and consistency between the background ($\vec{u}_b$) and hybrid ($\vec{u}_s$, $\vec{u}_c$) wavefields. In the case that the binding is in order (conditions applied correctly), it allows us to see the difference in the nature of the $\vec{u}_b$ wavefield (recorded in first step) on one side and both, $\vec{u}_c$ and $\vec{u}_s$ wavefields (computed in second step), on the other side. However, this does not mean that either of the wavefields are computed in a correct way in terms of wave propagation. For example, the FD–FD replication test, where $\vec{u}_b$ and $\vec{u}_c$ are both computed in the same 3-D inhomogeneous medium model, by the same FD method, and on a grid with the same design (time step, grid step, identical EB points in space and time) will provide a 'perfect' replication test with negligible errors.

In numerical applications, the thickness of the EB is non-zero to realize the boundary conditions in a straightforward way. It is limited by the design of the numerical approximation (e.g. FD template) and number of gridpoints per wavelength. For example, in FD second-order displacement formulation it is one-grid step thick (Opršal & Zahradník 2002), in staggered grid fourth order it is two grid steps (three grid lines) for each of the components and these are staggered (for more see Robertsson & Chapman 2000). However the background field can be (depending on the methods) computed exactly in the spatial and temporal points of the second-step FD grid design. That means that the FD-FD hybrid using the same FD method introduces only really minimal discrepancies shown in the replication test, where the complete wavefield relative error is less then 10^{-7} in terms of amplitude. Approximately the same value of 10^{-7} is given by the amplitude ratio between the scattered and the complete wavefields. In that sense the AK hybrid combination can be called 'perfect'. A combination of factors such as different wave propagation methods (ray-FD hybrid), different spatial and temporal coverage at the EB, different rheology/attenuation models and a different medium outside the EB may affect the accuracy. More details are given in Opršal & Zahradník (2002).

The duration of the excitation should cover the whole part of significantly large energy waves or amplitudes arriving at the whole EB. In the case of direct ray propagation in homogeneous medium to the site from a point source, with a simple and short source time function, it is practically a short pulse. In the case of a shallow source and method providing surface waves it may require a longer excitation time (Opršal & Zahradník 2002; Opršal *et al.* 2002). Tapering and cutting off the low-amplitude *P*-wave part (starting excitation with *S*-wave arrival to the EB) or tapering a too lengthy excitation is a possibility to save the computation time (Opršal *et al.* 1998, 1999) but abrupt cuts or too steep tapering may lead to artefact waves generated at the EB.

3 DISCUSSION AND CONCLUSIONS

The main result of this paper is a derivation of the condition common to a large group of methods given in Section 2.5. Eqs (6)–(9) describe a general boundary condition for the Alterman & Karal (1968) principle of wavefield injection, which is summarized by eqs (10)–(13). The eqs (10)–(13) describe the co-existence of the scattered (inside the EB) and the complete (outside the EB) wavefields, satisfying a single elastodynamic equation, while the boundary condition between these two wavefields is given by a discontinuity of the traction and displacement on the EB. At the same time that displacement discontinuity is equal to the background wavefield and satisfies the same elastodynamic equation on the EB.

The special or purely technical approaches are described by a common general condition on the wavefield injection boundary based on two independent wavefields and their difference. The condition is applicable to arbitrary combination of the two hybrid step methods based on the Alterman & Karal (1968) principle. The discontinuity between the scattered and complete wavefields can be naturally expressed by the displacement, stress or traction of the background wavefield applied in the equivalent approaches used so far. As a formal extension the main principle is describing both Bielak & Christiano (1984) and Alterman & Karal (1968) approaches.

The AK-principle based methods have a fully permeable excitation box (see Section 2.1) for the scattered wavefield, hence it can naturally propagate through the EB. The computed scattered wavefield is not 'hard prescribed' and is linearly separable, thanks to the known background wavefield, from the complete wavefield on the excitation box.

The AK method is directly applicable to linear problems—literally the problem has to be linear outside and on the excitation box, where simple addition and subtraction of the wavefield is performed when implemented (see conditions 22 and 6). The demand for linearity outside the EB arises from the fact that only the scattered wavefield is computed outside the EB in the second step and thus its non-linear interaction with the background wavefield is not possible. The model inside the excitation box may be non-linear because the computed wavefield is complete (u_c) there.

Advantages of the AK method can be summarized as follows. Since the general description given in (6), (20) and (22) does not limit the use of actual implementations, we believe that it also can combine other methods because the boundary condition, as it is, can be expanded to a zone-description (e.g. Bielak *et al.* 2003). As mentioned in Opršal & Zahradník (2002, section 3.1.2.2.), the condition virtually means a 'maintenance' of time-dependent discontinuity between the complete and scattered wavefields (being time-dependent as well), called the background wavefield, on the

© 2008 The Authors, *GJI*, **176,** 555–564
Journal compilation © 2008 RAS

excitation boundary. The same philosophy dates back to work by Herrera & Bielak (1977) who established conditions for traction and displacement discontinuity at the soil-structure interface adjacent to free surface, and is continued in Bielak & Christiano (1984), Cremonini *et al.* (1988) and Bielak *et al.* (2003).

In a general case, the medium at the excitation boundary (and its vicinity; for example one grid step in second-order FD use) always has to be linear to be able to generally apply the AK method. Possible non-linearity at the excitation box may be avoided, for example, in the case when the excitation signal duration is very short and thus the background wavefield is already zero at the time when a scattered wavefield of significantly enhanced amplitudes of non-linear field travels through the excitation box. Lecomte (1996) and Lecomte *et al.* (2004) describe a similar situation while avoiding the reflection of the scattered wavefield by their excitation box formulation.

Some advantages of the AK method are:

(i) Computations of background wavefield generated by complex-source (finite-extend, dynamic) are performed separately from site-effects (complete wavefield).

(ii) Repeated computations of the second step in parametric study or waveform inversion. The excitation (background wavefield) is the same while model alterations are done for each of multiple second-step computations.

(iii) Source-site distance may be very large, the second-step model can be (depending on the situation) a very small fraction of the whole model and thus computation may be done up to engineering frequencies (Opršal & Fäh 2007, 0–12 Hz).

(iv) The first step is typically computed for a relatively simple medium.

(v) Easy parallelization of (e.g. FD or FE) second-step computations.

(vi) Reducing computer memory and time requirements

(vii) Relatively small values of the scattered wavefield (computed outside the EB, practically equal to zero in a successful replication test) compared to the direct all-in-one incoming wavefield. Hence the spurious reflections from the absorbing boundaries are also smaller.

(viii) Relatively simple implementation of canonical excitations like planar or spherical wave of arbitrary incidence angle and polarization.

ACKNOWLEDGMENTS

The manuscript benefited from helpful comments of the editor Jean Virieux and two anonymous reviewers. The authors would like to thank Clive A. Cowan (CCR) for critical reading and Jiří Zahradník for useful comments that greatly improved this manuscript. This research was supported by the projects: Czech National Foundation under the grant No. 205/07/0502, the Research project MSM0021620860 of the Czech Ministry of Education and Japanese Society for Promotion of Science award FY2006/P06320.

REFERENCES

Alterman, Z. & Karal, F.C., 1968. Propagation of elastic waves in layered media by finite-difference methods, *Bull. seism. Soc. Am.,* **58,** 367–398.

Bamberger, A., Enquist, B., Halpern, L. & Joly, P., 1986. Higher order paraxial wave equation approximations in heterogeneous media. INRIA, research report No 558.

Bielak, J., 2005. Reply to "Comment on 'domain reduction method for three-dimensional earthquake modeling. . .", *Bull. seism. Soc. Am.,* **95,** 770–773.

Bielak, J. & Christiano, P., 1984. On the effective seismic input for nonlinear soil structure interaction systems, *Earthq. Eng. Struct. Dyn.,* **12,** 107–119.

Bielak, J., Loukakis, K., Hisada, Y. & Yoshimura, C., 2003. Domain reduction method for three-dimensional earthquake modeling in localized regions. Part I: theory, *Bull. seism. Soc. Am.,* **93,** 817–824.

Caserta, A., Zahradník, J. & Plicka, V., 1999. Ground motion modeling with a stochastically perturbed excitation, *J. Seismol.,* **3,** 45–59.

Cremonini, M.G., Christiano, P. & Bielak, J., 1988. Implementation of effective seismic input for soil-structure interaction systems. *Earthq. Eng. Struct. Dyn.,* **16,** 615–625.

De Martin, F., Modaressi, H. & Aochi, H., 2007. Coupling of FDM and FEM in seismic wave propagation, in *Proceedings of 4th International Conference on Earthquake Geotechnical Engineering June 25–28, 2007*, Greece, Paper No. 1743, 12pp.

Faccioli, E., Vanini, A., Paolucci, R. & Stupazzini, A., 2004. Comment on Domain reduction method for three-dimensional earthquake modeling in localized regions, Part 1: theory, "by J. Bielak, K., Loukakis, Y. Hisada, and C. Yoshimura, and " Part II: verification and applications, " by C. Yoshimura, J., Bielak, Y. Hisada, and A. Fernandez, *Bull. seism. Soc. Am.,* **95,** 763–769.

Fäh, D., 1992. A hybrid technique for the estimation of strong ground motion in sedimentary basins, *PhD thesis*, Diss. ETH Nr. 9767, Swiss Federal Institute of Technology, Zurich.

Fäh, D., Suhadolc, P, & Panza, G.F., 1990. Estimation of strong ground motion in laterally heterogeneous media: Modal summation– finite differences, in *Proceedings of the 9th European Conf. of Earthquake Engineering, 11–16 September*, Moscow, USSR,Vol. 4A, pp. 100–109.

Fäh, D., Suhadolc, P. & Panza, G.F., 1993. Variability of seismic ground motion in complex media: the case of a sedimentary basin in the Friuli (Italy) area, *J. appl. Geophys.,* **30,** 131–148.

Fäh, D., Suhadolc, P., Mueller, St. & Panza, G.F., 1994. A hybrid method for the estimation of ground motion in sedimentary basins: quantitative modeling for Mexico City, *Bull. seism. Soc. Am.,* **84**(2), 383–399.

Fäh, D. et al., 2006. The earthquake of 250 A.D. in Augusta Raurica, A real event with a 3D site-effect? *J. Seismol.,* doi:10.1007/s10950-006-9031-1, 19pp.

Gazetas, G., Kallou, P.V. & Psarropoulos, P.N., 2002. Topography and soil effects in the MS 5.9 Parnitha (Athens) earthquake: the case of Adámes, *Nat. Hazards,* **27,** 133–169.

Gjøystdal, H., Iversen, E., Laurain, R., Lecomte, I., Vinje, V. & Åstebøl, K., 2002. Review of ray theory applications in modelling and imaging of seismic data. *Stud. Geophys. Geod.,* **46,** 113–164.

Gjøystdal, H., Lecomte, I., Mjelva, A.E., Maaø, F., Hokstad, K. & Johansen, T.A., 1998. Fast repeated seismic modelling of local complex targets. *Expanded Abstracts, 68th SEG Annual Meeting,* 1452–1455.

Hatayama, K., 2006. Long-Period Strong Ground Motions in Tomakomai during the 2003 Tokachi-oki Earthquake: (3) Effects of Basin Planar shape (in Japanese), in *Proceedings of the Seismological Society of Japan, Fall Meeting, Oct 31–Nov 1, 2006*, Nagoya, Japan, talk D033, pp. 135–135.

Hatayama, K., Kanno, T. & Kudo, K., 2007. Control factors of spatial variation of long-period strong ground motions in the Yufutsu Sedimentary Basin, Hokkaido, during the Mw 8.0 2003 Tokachi-oki, Japan, Earthquake, *Bull. seism. Soc. Am.,* **97,** 1308–1323.

Helmberger, D.V. & Vidale, J.E., 1988. Modeling strong motions produced by earthquakes with two-dimensional numerical codes. *Bull. seism. Soc. Am.,* **78,** 109–121.

Herrera, I. & Bielak, J., 1977. Soil-structure interaction as a diffraction problem, in *Proceedings of the 6th World Conf. on Earthquake Eng.*, New Delhi, pp. 19–24.

Hestholm, S., Moran, M., Ketcham, S., Anderson, T., Dillen, M. & McMechan, G., 2006, Effects of free-surface topography on moving-seismic-source modeling, *Geophysics,* **71,** 159–166, doi:10.1190/1.2356258.

Hokstad, K., Lecomte, I., Maaø, F., Tuseth, M., Mjelva, A.E., Gjøystdal, H. & Sollie, R., 1998. Hybrid modelling of elastic wavefield propagation, *Extended Abstracts, 60th EAGE Annual Meeting,* 5–56.

Kelly, K.R., Ward, R.W., Treitel, S. & Alford, R.M., 1976. Synthetic seismograms: A finite-difference approach. *Geophysics,* **41,** 2–27.

Kontoe, S., Zdravkovic, L. & Potts, D.M., 2008a. The Domain Reduction Method for dynamic coupled consolidation problems in geotechnical engineering, *Int. J. Numer. Anal. Methods Geomech.,* **32**(6), 659–680.

Kontoe, S., Zdravkovic, L. & Potts, D.M., 2008b. An assessment of the domain reduction method as an advanced boundary condition and some pitfalls in the use of conventional absorbing boundaries, *Int. J. Numer. Anal. Meth. Geomech.,* doi:10.1002/nag.713.

Lecomte I., 1996. Hybrid modelling with ray tracing and finite difference, *66th Ann. Internat. Mtg: Soc. of Expl. Geophys.,* 699–702.

Lecomte, I., Gjøystdal, H., Maaø, F., Bakke, R., Drottning, Å. & Johansen, T.-A., 2004. Efficient and flexible seismic modelling of reservoirs: the HybriSeis concept, *Leading Edge,* **23,** 432–437.

Levander, A.R., 1989. Finite-difference forward modeling in seismology, in *The Encyclopedia of Solid Earth Geophysics*, pp. 410–431, ed. James, D.E., Van Nostrand Reinhold.

Loukakis, K.E., 1988. Transient response of shallow-layered valleys for inclined incident SV waves calculated by the finite element method, *MSc. thesis*, Department of Civil Engineering, Carnegie Mellon University, Pittsburgh, Pennsylvania.

Loukakis, K. & Bielak, J., 1994. Seismic response of two-dimensional sediment-filled valleys to oblique incident SV-waves calculated by the finite element method, in *Proceedings of the 5th U.S. National Conf. Earthquake Eng.*, Chicago, **Vol. 3,** pp. 25–34.

Modaressi, H., 1987. Modélisation numérique de la propagation des ondes dans les milieux poreux anélastiques, *PhD thesis*, Ecole Centrale Paris, France.

Moczo, P., 1989. Finite-difference technique for SH-waves in 2-D media using irregular grids—application to the seismic response problem, *Geophys. J. Int.,* **99,** 321–329.

Moczo, P., Bystricky, E., Kristek, J., Carcione, J.M. & Bouchon, M., 1997. Hybrid modeling of P-SV seismic motion at inhomogeneous viscoelastic topographic structures, *Bull. seism. Soc. Am.,* **87,** 1305–1323.

Moczo, P., Kristek, J., Gális, M., Pazak, P. & Balazovjech, M., 2007a. The finite-difference and finite-element modeling of seismic wave propagation and earthquake motion, *Acta Phys. Slovaca,* **57**(2), 177–406.

Moczo, P., Robertsson, J.O.A. & Eisner, L., 2007b. The finite-difference time-domain method for modelling of seismic wave propagation, in *Advances in Wave Propagation in Heterogeneous Earth, Advances in Geophysics 48*, pp. 421–516, eds Wu, R.-S., Maupin, V. & Dmowska, R., Elsevier - Academic Press, New York.

Olsen, K.B., Nigbor, R. & Konno, T., 2000. 3D viscoelastic wave propagation in the Upper Borrego Valley, California, constrained by borehole and surface data, *Bull. seism. Soc. Am.,* **90,** 134–150.

Opršal, I. & Fäh, D., 2007. 1D vs 3D strong ground motion hybrid modelling of site, and pronounced topography effects at Augusta Raurica, Switzerland—earthquakes or battles? *Proceedings of 4th International Conference on Earthquake Geotechnical Engineering June 25–28, 2007, Greece*, Paper No. 1416, 12pp.

Opršal, I. & Zahradník, J., 2002. Three-dimensional finite difference method and hybrid modeling of earthquake ground motion, *J. geophys. Res.,* **107**(B8), 16pp., doi:10.1029/2000JB000082.

Opršal, I., Brokešová, J., Fäh, D. & Giardini, D., 2002. 3D Hybrid Ray-FD and DWN-FD Seismic modeling for simple models containing complex local structures, *Stud. Geophys. Geod.,* **46,** 711–730.

Opršal, I., Fäh, D., Mai, M. & Giardini, D., 2005. Deterministic earthquake scenario for the Basel area: Simulating strong motions and site effects for Basel, Switzerland, *J. geophys. Res.,* **110**(B4), B04305, doi:10.1029/2004JB003188, 19pp.

Opršal, I., Pakzad, M., Plicka, V. & Zahradník, J., 1998. Ground motion simulation by hybrid methods, in *The Effects of Surface Geology on Seismic Motion, Proceedings of ESG'98, December 1–3, 1998*, Yokohama, Japan, Balkema, Rotterdam, eds Irikura, K. Kudo, H. Okada & T. Sasatani, ISBN 90 5809 032 9 (Vol. 2), pp. 955–960.

Opršal, I., Plicka, V. & Zahradník, J., 1999. Kobe simulation by hybrid methods, in *The Effects of Surface Geology on Seismic Motion, Proceedings of ESG'98, December 1–3, 1998*, Yokohama, Japan, Balkema, Rotterdam, eds Irikura, K. Kudo, H. Okada & T. Sasatani, ISBN 90 5809 033 7 (Vol. 3), pp. 1451–1456.

Opršal, I., Zahradník, J., Serpetsidaki, A. & Tselenits, G.-A., 2004. 3D hybrid simulation of the source and site effects during the 1999 Athens earthquake, in *Proceedings of 13th World Conference on Earthquake Engineering, August 1–6, 2004*, Vancouver, B.C., Canada, Paper No. 3337, 15 pp.

Pitarka, A. & Irikura, K., 1996. Basin structure effects on long-period strong motions in the San Fernando Valley and the Los Angeles basin from the 1994 Northridge earthquake and an aftershock, *Bull. seism. Soc. Am.,* **86**(1B), S126–S137.

Pitarka, A.S., Takenaka, H. & Suetsugu, D., 1994. Modeling strong motion in the Ashigara valley for the 1990 Odawara, Japan, earthquake, *Bull. seism. Soc. Am.,* **84,** 1327–1335.

Pitarka, A., Suetsugu, D. & Takenaka, H., 1996. Elastic finite-difference modeling of strong motion in Ashigara valley for the 1990 Odawara, Japan, earthquake, *Bull. seism. Soc. Am.,* **86,** 981–990.

Riepl, J., 1997, Effets de site: évaluation experimentale et modélisations multidimensionnelles: application au site test EURO-SEISTEST (Grèce). *Thèse*, L'Université Joseph Fourier de Grenoble.

Riepl, J., Zahradník, J., Plicka, V. & Bard, P.-Y., 2000. About the efficiency of numerical 1D and 2D modeling of site effects in basin structures, *Pure appl. Geophys.,* **157,** 319–342.

Robertsson, J.O.A. & Chapman, C.H., 2000. An efficient method for calculating finite-difference seismograms after model alterations, *Geophysics,* **65,** 907–918.

Robertsson, J.O.A., Levander, A. & Holliger, K., 1996. A hybrid wave propagation simulation technique for ocean acoustic problems, *J. geophys. Res.,* **101,** 11 225–11 241.

Robertsson, J.O.A., Ryan-Grigor, S., Sayers, C. & Chapman, C.H., 2000. A finite-difference injection approach to modeling of seismic fluid flow monitoring, *Geophysics,* **65,** 896–906.

Sorensen, M.B., Opršal, I., Bonnefoy-Claudet, S., Atakan, K., Mai, P.M., Pulido, N. & Yalciner, C., 2006. Local site effects in Ataköy, Istanbul, Turkey, due to a future large earthquake in the Marmara Sea, *Geophys. J. Int.,* **167,** 1413–1424, doi:10.1111/j.1365-246X.2006.03204.x.

Stupazzini, M., Zambelli, C., Massidda, L., Paolucci, R., Maggio, F.3. & di Prisco, C., 2006. The spectral element method as an effective tool for solving large scale dynamic soil-structure interaction problems, in *Proceedings of the 8th U.S. National Conference on Earthquake Engineering April 18–22, 2006, San Francisco*, California, USA, Paper No. 413, 10pp.

Takeuchi, N., 1996. A new method for computing highly accurate synthetic seismograms, *DSc thesis,* Tokyo University.

Takeuchi, N. & Geller, R.J., 2003. Accurate numerical methods for solving the elastic equation of motion for arbitrary source locations. *Geophys. J. Int.,* **154,** 852–866.

Takenaka, H., Ohshima, M. & Okamoto, T., 2006. An effective non-reflecting side-boundary technique for plane- wave incidence in 2D or 2.5D FDM computations: real-time use of full elastic 1D scheme, S41B-1326, *AGU Fall Meeting*, San Francisco, December 11–15, 2006.

Vidale, J.E. & Helmberger, D.V., 1987. Path effects in strong motion seismology, in *Seismic Strong Motion Synthetics*, pp. 267–319, ed. Bolt, B.A., Academic Press, Orlando, FL, USA.

Vidale, J.E. & Helmberger, D.V., 1988. Elastic Finite-difference Modeling of the 1971 San Fernando, California Earthquake. *Bull. seism. Soc. Am.,* **78**(1), 122–141.

Vidale, J.E., Helmberger, D.H. & Clayton, R.W., 1985. Finite- difference seismograms for SH waves, *Bull. seism. Soc. Am.,* **75,** 1765–1782.

Xu, H., Day, S.M. & Minster, J.-B.H., 1999. Two-dimensional linear and nonlinear wave propagation in a half-space, *Bull. seism. Soc. Am.,* **89,** 903–917.

Yang, Z., He, L., Bielak, J., Zhang, Y., Elgamal, A. & Conte, J., 2003. Nonlinear seismic response of a bridge site subjected to spatially varying

ground motion, in *Proceedings of the 16th ASCE Engineering Mechanics Conference, July 16–18*, Univ. of Washington, Seattle, WA., Paper No. GL0992, 7pp.

Yoshimura, C., 2003. Sanjigen fuseikei jiban ni okeru jishin hado denpa ni kansuru kenkyu (in Japanese; Seismic wave propagations in three-dimensional irregular grounds), *PhD thesis*, Waseda University, Japan, (2003/3/24), 137pp.

Yoshimura, C., Bielak, J., Hisada, Y. & Fern´andez, A., 2003. Domain reduction method for three-dimensional earthquake modeling in localized regions. Part II: verification and applications. *Bull. seism. Soc. Am.* **93,** 825–840.

Zahradník, J., 1995. Comment on "a hybrid method for the estimation of ground motion in sedimentary basins' quantitative modeling for Mexico City" by D. Fäh, P., Suhadolc, St. Mueller, and G. F. Panza, *Bull. seism. Soc. Am.,* **85**(4), 1268–1270.

Zahradník, J. & Moczo, P., 1996. Hybrid seismic modelling based on discrete-wave number and finite-difference methods, *Pure appl. Geophys.,* **148,** 21–38.